

Federated Distillation Assisted Vehicle Edge Caching Scheme Based on Lightweight DDPM

Xun Li, Qiong Wu, *Senior Member, IEEE*, Pingyi Fan, *Senior Member, IEEE*,
 Kezhi Wang, *Senior Member, IEEE*, Wen Chen, *Senior Member, IEEE*, and Khaled B. Letaief, *Fellow, IEEE*

Abstract—Vehicle edge caching is a promising technology that can significantly reduce the latency for vehicle users (VUs) to access content by pre-caching user-interested content at edge nodes. It is crucial to accurately predict the content that VUs are interested in without exposing their privacy. Traditional federated learning (FL) can protect user privacy by sharing models rather than raw data. However, the training of FL requires frequent model transmission, which can result in significant communication overhead. Additionally, vehicles may leave the road side unit (RSU) coverage area before training is completed, leading to training failures. To address these issues, in this letter, we propose a federated distillation-assisted vehicle edge caching scheme based on lightweight denoising diffusion probabilistic model (LDPM). The simulation results demonstrate that the proposed vehicle edge caching scheme has good robustness to variations in vehicle speed, significantly reducing communication overhead and improving cache hit percentage.

Index Terms—Denoising diffusion probabilistic model, federated distillation, edge caching.

I. INTRODUCTION

WITH the rapid growth of demand for autonomous driving and vehicle networking, vehicles need to obtain map navigation data and multimedia content in real-time to improve driving efficiency and experience [1], [2]. Vehicle edge caching technology, by pre-caching content of interest to vehicle users (VUs) in roadside units (RSUs), can significantly reduce content request latency and core network pressure [3], [4]. However, the cache capacity of RSUs is limited, so it

is crucial to accurately predict the content that users are interested in.

Denoising diffusion probabilistic model (DDPM) has received widespread attention due to its outstanding generative performance [5]. User data is usually sparse because users only rate a limited number of items. DDPM can learn the distribution of user data and generate high-quality samples to fill in the unrated items [6]. Applying DDPM to edge caching can achieve more accurate content prediction to a certain extent, enabling vehicles to obtain content that better meets their needs at RSUs. However, the training and deployment of DDPM require substantial computational resources, making them unsuitable for resource-constrained vehicle environments. The lightweight U-Net architecture of the DDPM has been proven to effectively reduce its demand for computing resources [7], [8]. Therefore, adopting a lightweight DDPM (LDPM) is an effective solution. However, model training still requires users' personal data, which raises privacy concerns. Federated learning (FL) can protect user privacy by sharing local models rather than raw data [9], [10]. Nevertheless, each round of iteration in FL requires the transmission of full model parameters between vehicles and the server, which incurs significant communication overhead [11], [12].

Moreover, the high mobility of vehicles also poses significant challenges to edge caching. Vehicles may leave the coverage area of the RSU before the model training is completed, resulting in the failure of model training. Previous methods usually perform vehicle selection before training to ensure that training can be completed [13], [14]. However, this is not applicable to scenarios with slow model convergence, large amounts of local data, and large model sizes. The mobility of vehicles has greatly restricted the application of vehicle edge caching.

To address these issues, in this letter, we propose a federated distillation-assisted vehicle edge caching scheme based on LDPM¹. The main innovations of this letter are as follows: 1) We propose a new federated distillation algorithm suitable for vehicle edge caching, which significantly reduces communication overhead compared with previous algorithms. 2) We combine DDPM with the distillation algorithm and apply them to vehicle edge caching, which improves the cache hit percentage.

This work was supported in part by Jiangxi Province Science and Technology Development Programme under Grant 20242BCC32016; in part by the National Natural Science Foundation of China under Grant 61701197; in part by Basic Research Program of Jiangsu under Grant BK20252084; in part by the National Key Research and Development Program of China under Grant 2021YFA1000500(4); in part by the Research Grants Council under the Areas of Excellence Scheme under Grant AoE/E-601/22-R; and in part by the 111 Project under Grant B23008. (Corresponding author: Qiong Wu.)

Xun Li and Qiong Wu are with the School of Internet of Things Engineering, Jiangnan University, Wuxi 214122, China, and also with the School of Information Engineering, Jiangxi Provincial Key Laboratory of Advanced Signal Processing and Intelligent Communications, Nanchang University, Nanchang 330031, China (e-mail: xunli@stu.jiangnan.edu.cn; qiongwu@jiangnan.edu.cn).

Pingyi Fan is with the Department of Electronic Engineering, State Key Laboratory of Space Network and Communications, and the Beijing National Research Center for Information Science and Technology, Tsinghua University, Beijing 100084, China (e-mail: fpy@tsinghua.edu.cn).

Kezhi Wang is with the Department of Computer Science, Brunel University, London, Middlesex UB8 3PH, U.K (e-mail: Kezhi.Wang@brunel.ac.uk).

Wen Chen is with the Department of Electronic Engineering, Shanghai JiaoTong University, Shanghai 200240, China (e-mail: wenchen@sjtu.edu.cn).

Khaled B. Letaief is with the Department of Electrical and Computer Engineering, the Hong Kong University of Science and Technology, Hong Kong (e-mail: eekhaled@ust.hk).

¹The source code has been released at: <https://github.com/qiongwu86/Federated-Distillation-Assisted-Vehicle-Edge-Caching-Scheme-Based-on-Lightweight-DDPM>

II. SYSTEM MODEL

A. System Scenario

We consider a highway system scenario as illustrated in Fig. 1, where the vehicle edge computing network consists of three layers: a macro base station (MBS), RSUs, and vehicles. Each RSU $r = 1, 2, \dots, R$ is connected to the MBS via a reliable wired link, and vehicles $i = 1, 2, \dots, I$ are located within the coverage area of the RSUs. Each vehicle has its own local data d_i , and is equipped with a communication module, a distillation module, and locally pre-trained encoder and decoder networks. The speed of each vehicle follows an independent and identically distributed truncated Gaussian distribution. Let V_i^r denote the speed of vehicle i under r -th RSU, then the probability density function $f(V_i^r)$ of V_i^r is expressed as [15]

$$f(V_i^r) = \begin{cases} \frac{2e^{-\frac{1}{2\sigma^2}(V_i^r - \mu)^2}}{\sqrt{2\pi\sigma^2}(erf(\frac{V_{\max} - \mu}{\sigma\sqrt{2}}) - erf(\frac{V_{\min} - \mu}{\sigma\sqrt{2}}))} & V_{\min} \leq V_i^r \leq V_{\max}, \\ 0 & \text{otherwise,} \end{cases} \quad (1)$$

where V_{\max} and V_{\min} are the maximum and minimum speed thresholds of the vehicle, and $erf(\frac{V_i^r - \mu}{\sigma\sqrt{2}})$ is the Gaussian error function with mean μ and variance σ^2 .

Each RSU is equipped with a communication module, a caching module, and a knowledge caching (KC) module. The KC module consists of a hash-to-index (HI) module and a knowledge-to-index (KI) module. The HI module and KI module are used to store the HI pairs and KI pairs uploaded by the vehicles, respectively. The caching module has limited caching capacity, capable of caching at most N pieces of content. We assume that the MBS stores all available content. When the content requested by a vehicle is cached in the RSU, the RSU directly delivers the content to the vehicle. Otherwise, the RSU requests the content from the MBS before delivering it to the vehicle, which results in higher content request latency. Our goal is to reduce the latency for VUs to access content by accurately predicting the content of interest to VUs and pre-caching it at the RSUs, thereby maximizing the cache hit percentage of the cached content.

B. Denoising Diffusion Probabilistic Model (DDPM)

DDPM transform original data into Gaussian noise through the forward diffusion process, and then recover the original data through the reverse generation process. The forward process of the DDPM parameterizes the Markov chain using a dynamic scheduling policy $\{\beta_t\}_{t=1}^T$, gradually adding Gaussian noise to the original data, causing the data distribution to gradually approach random noise perturbation, where T is the number of time steps. The reverse diffusion process of the DDPM gradually denoises the noise to restore the original data distribution.

The LDPM we adopt mainly focuses on the lightweighting of its U-Net architecture. The U-Net architecture is similar to [16]. The main differences are the replacement of 2D convolutions with 1D convolutions to adapt to the structure of user interaction data, and the use of a quarter of the channel

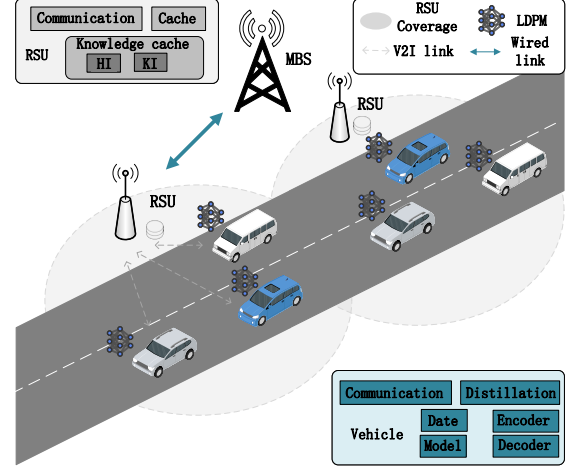


Fig. 1. System Model.

numbers and three feature map resolutions to reduce the model size [17], [18]. Therefore, the LDPM has a parameter count of only 770K, making it suitable for the vast majority of vehicles. In [19], Ho *et al.* proposed a simplified objective function for optimization, expressed as

$$\mathcal{L}_{t-1}^{simple} = \mathbb{E}_{t, \mathbf{x}_0, \epsilon \sim \mathcal{N}(0, \mathbf{I})} \left[\left\| \epsilon - \epsilon_\theta \left(\sqrt{\alpha_t} \mathbf{x}_0 + \sqrt{1 - \alpha_t} \epsilon, t \right) \right\|^2 \right]. \quad (2)$$

Here, \mathbf{x}_0 represents the data at time step 0, ϵ_θ is the neural network to be trained, $\bar{\alpha}_t = \prod_{i=1}^t \alpha_i$ and $\alpha_t = 1 - \beta_t$.

III. VEHICLE EDGE CACHING SCHEME

To address the challenges brought by the high-speed movement of vehicles and the significant communication overhead caused by model training in traditional methods, we propose a vehicle edge caching scheme. Specifically, this scheme includes the execution process between vehicles and RSUs, and the execution process between RSUs and MBS. We will describe it in the following parts.

A. Execution between Vehicles and RSUs

Each vehicle i will upload its content recommendation list $L_{i,r}$ when entering r -th RSU. The content recommendation list is generated by the vehicle using local models. The execution between the RSUs and the vehicles is shown in Fig. 2, which includes the following steps:

1) *Hash Encoding and Uploading*: Each vehicle uploads the HI pair to the RSU. The HI pair consists of a hash code h_i^r and a vehicle index i , where h_i^r represents the hash code of vehicle i in the r -th RSU. The hash code h_i^r is generated by the vehicle locally using a pre-trained encoder $E_i(\cdot)$ to encode their local data d_i , i.e.

$$h_i^r = E_i(d_i). \quad (3)$$

The pre-encoder is designed as a deep neural network, and its output dimension is much smaller than that of the original data, thus sharing hash code with RSU ensures privacy and also having low communication overhead. Pre-trained encoder and pre-trained decoder are trained using publicly available datasets and then fine-tuned with local data [20].

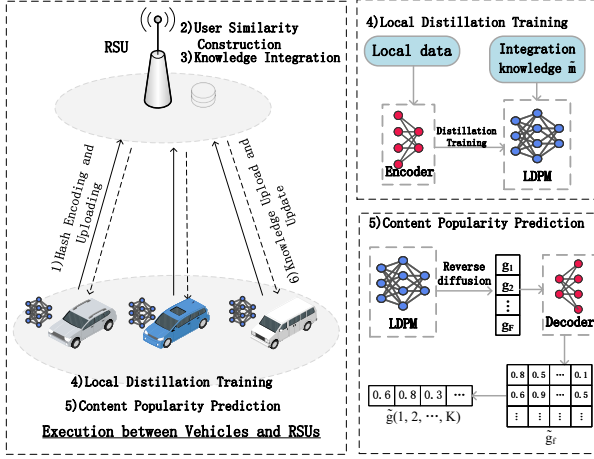


Fig. 2. Execution between Vehicles and RSUs.

2) *User Similarity Construction*: Unlike [21], we calculate the similarity between users rather than individual samples. The main reason for this is that users only rate a limited number of items, which results in their data containing many zero values. Directly calculating the similarity between each sample would treat these unrated items as content that VUs are not interested in, leading to a biased prediction [13]. After the RSU receives the HI pair uploaded by vehicle i , it immediately saves or updates the corresponding content in the HI module,

$$HI(i, r) \leftarrow (h_i^r, i). \quad (4)$$

Since vehicles with similar preferences are mapped to hash code vectors with similar directions, the C neighboring vehicles with the most similar preferences to vehicle i can be found by calculating the cosine similarity between the HI of vehicles [22], i.e.

$$\begin{aligned} & \underset{s_1, s_2, \dots, s_C}{\operatorname{argmax}} \sum_{c=1}^C \cos(HI(i, r), HI(s_c, r)), \\ & \text{s.t. } \cos(HI(i, r), HI(s_c, r)) \geq \gamma, s_c \neq i, \end{aligned} \quad (5)$$

where γ is the minimum threshold for user similarity.

3) *Knowledge Integration*: The RSU extracts knowledge $(m_i^r)_c$ from the KC for the C neighboring users of vehicle i . Then, this knowledge is averaged to obtain aggregated knowledge \tilde{m}_i^r that reflects the overall preferences of neighboring users, subsequently passing it to the corresponding vehicle,

$$(m_i^r)_1, (m_i^r)_2, \dots, (m_i^r)_C = KC(h_i^r, i, r), \quad (6)$$

$$\tilde{m}_i^r = \frac{1}{C} \sum_{c=1}^C (m_i^r)_s, \quad (7)$$

where $(m_i^r)_c$ is the knowledge of the c -th similar user of vehicle i in r -th RSU.

4) *Local Distillation Training*: In this step, each vehicle i uses local data and acquired integrated knowledge to conduct local distillation training. Since latent-space training with LDPM can significantly reduce the required computational resources and accelerate training efficiency [20]. We map the original data d_i to a low-dimensional latent space $\hat{d}_i = E_i(d_i)$

before training. The local LDPM is then trained in this low-dimensional latent space. For each data \hat{z} in \hat{d}_i , the optimization function for local distillation training is calculated as

$$\begin{aligned} \arg \min_{\omega_i} J^i(\omega_i) = \arg \min_{\omega_i} \sum_{\hat{z} \in \hat{d}_i} & \left[\mathcal{L}(\omega_i; \hat{z}) \right. \\ & \left. + \lambda \text{KL}(o(g_i^r; \delta) \parallel o(\tilde{m}_i^r; \delta)) \right]. \end{aligned} \quad (8)$$

The first part is the original training loss of the local model for its own samples, where ω_i is the local LDPM parameter; the second part is the KL divergence term that incorporates integrated knowledge into training, where δ is the temperature parameter of the softmax function $o(\cdot)$, λ is the weight factor, and g_i^r is the output of the local model [21].

5) *Content Popularity Prediction*: After completing the local distillation training, each vehicle i uses the local LDPM to perform the reverse diffusion process, generating F sample data points $g_{i,f}^r$, where F is the number of sample data points and $f = 1, 2, \dots, F$. These sample data points are mapped to the original data dimension via the pre-trained decoder to obtain the reconstructed sample data $\tilde{g}_{i,f}^r = D(g_{i,f}^r)$, where $D(\cdot)$ represents the decoder network. These reconstructed data are used for content popularity prediction. Compared to the original data, these reconstructed data better reflect VUs' preferences for content because they contain fewer zero values. Assuming there are a total of K content items, the dimension of $\tilde{g}_{i,f}^r$ is K and can be expressed as $\tilde{g}_{i,f}^r(1, 2, \dots, K)$. All reconstructed data can be added by dimension to obtain the score $\tilde{g}_i^r(1, 2, \dots, K)$ of all contents,

$$\tilde{g}_i^r(1, 2, \dots, K) = \frac{1}{F} \sum_{f=1}^F \tilde{g}_{i,f}^r(1, 2, \dots, K). \quad (9)$$

The score $\tilde{g}_i^r(1, 2, \dots, K)$ reflects the preferences of VU i . The higher the score, the more interested the VU is. Then, select the top M items as the VU's new content recommendation list $L_{i,r}$.

6) *Knowledge Upload and Update*: The vehicle uploads KI pair and the new content recommendation list to the RSU. The KI pair is constructed using the vehicle index i and the model output knowledge $g_{i,f}^r$,

$$KI(i, r) \leftarrow (g_{i,f}^r, i). \quad (10)$$

Subsequently, the RSU updates the KI module to ensure that the latest knowledge can be retrieved for the next request. Since the dimension of the knowledge is much lower than that of the VU's original data, sharing the knowledge will not leak the VU's privacy and having low communication overhead.

B. Execution between RSUs and MBS

When vehicles within the coverage of an RSU uploads a content recommendation list, the RSU will update its cache content. Additionally, to prevent the information stored in KC module from becoming outdated after vehicles leave the RSU's coverage, the RSU periodically updates KC . The execution between the RSU and MBS are as follows:

TABLE I. Values of the parameters in the experiments.

Parameter	Value	Parameter	Value
T	50	δ	2
λ	1	K	3952
F	500	η	0.1

1) *Mobility-Aware Cache Replacement*: The RSU updates the cached content based on the content recommendation list uploaded by vehicles within its coverage. In addition, the position of the vehicle in the RSU and the vehicle speed factors should also be considered, as vehicles that stay in the RSU for a longer time are more likely to request more content, and their content recommendation list should be given greater weight. For each content k , its score $u_r(k)$ can be represented as

$$u_r(k) = \sum_{i \in \mathcal{U}_r} \eta \frac{B - P_i}{V_i^r} \mathbf{1}(k \in L_{i,r}), \quad (11)$$

where \mathcal{U}_r is the set of vehicles currently served by r -th RSU, P_i is the distance from vehicle i to the entrance of RSU, η is the location weight factor, B is the coverage range of RSU and $\mathbf{1}(\cdot)$ is an indicator function. The RSU caches the top N contents with the highest scores based on the scores of all contents.

2) *KC Update*: The RSU periodically uploads the content of its KC to the MBS. The MBS aggregates the KC of RSUs within its coverage area, retaining only the latest KC for each vehicle i based on their upload time. It then passes the updated KC_{lat} to the RSUs within its coverage area. The KC update process is as follows

$$r_i^* = \arg \max_{r \in \{1, \dots, R\}} t_{i,r}, \quad (12)$$

$$KC_{lat} = \bigcup_{i=1}^I \{KI(i, r_i^*), HI(i, r_i^*)\}, \quad (13)$$

where $t_{i,r}$ represents the time at which vehicle i uploads HI pair to the r -th RSU.

IV. SIMULATION

In this section, we introduce the experiments. The dataset is the widely-used MovieLens 1M, which includes 1,002,099 rating records from 6,040 users on 3,952 movies. These ratings range from 0 to 5. Some parameters of the experiments are shown in Table I. Unless otherwise specified, we set the cache capacity as 500 and the vehicle speed as 25 m/s. Additionally, to evaluate the performance of the schemes, we introduce cache hit percentage and request content latency [23]. Cache hit percentage indicates the probability of directly accessing the requested content from nearby RSU. If the requested content has been cached in advance, it is considered a successful cache; otherwise, it is a failure. Request content latency represents the average latency for all VUs to request content. We compare our scheme with other schemes, such as:

- Oracle [24]: This scheme possesses full prior knowledge of VUs' future requests, defining the theoretical maximum achievable cache hit percentage.

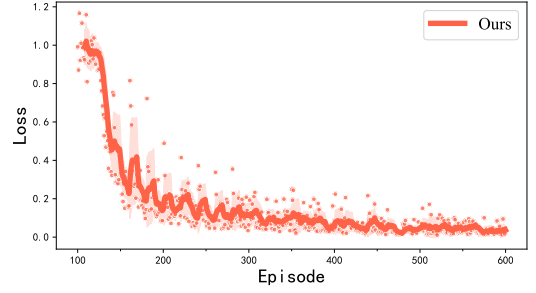


Fig. 3. Loss versus episodes.

- CAFR [13]: This scheme proposed the combination of asynchronous FL and autoencoder for edge caching, combined with a mobility aware mechanism, provides a feasible solution for vehicle edge caching.
- N- τ -greedy: This scheme selects the contents with the N largest request counts based on probability $1 - \tau$ and selects N contents randomly based on probability τ to cache. In the experiment, $\tau = 0.2$.
- FedAvg: This scheme combines traditional FL algorithm with LDPM, rather than the federated distillation algorithm.
- AsyFed: This scheme combines asynchronous FL with LDPM, instead of the federated distillation algorithm.

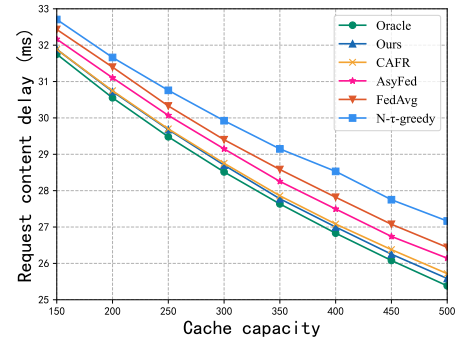


Fig. 4. Request content delay versus cache capacity.

Fig. 3 shows the convergence curve of model training, where it can be observed that the model loss gradually decreases with the increase in episodes, and the model converges at approximately 300 episodes.

As can be seen from Table II, with the cache capacity increases, the cache hit percentage of various schemes gradually rise. This is because a higher cache capacity allows the RSU to cache more content, making it more likely for VUs to request the desired content from the RSU. Oracle achieves the best performance because it knows the VUs' future requests, representing the theoretical optimal value. It can be seen that our scheme achieves the best performance except for Oracle, and this is because our scheme trains a personalized local LDPM for each VU, which can accurately predict the content each VU is interested in. AsyFed performs worse than CAFR, as it is difficult for AsyFed to complete training before high-speed moving vehicles leave the RSU. FedAvg is more severely affected by vehicle speed, thus

TABLE II. Cache hit percentage and communication overhead under different schemes.

Scheme	Cache capacity								Overhead (MB)
	150	200	250	300	350	400	450	500	
Ours	23.95%	29.13%	33.82%	38.19%	42.34%	45.81%	49.15%	52.14%	1.78
Oracle	24.54%	29.91%	34.71%	39.03%	42.97%	46.57%	49.93%	53.05%	-
CAFR	23.93%	29.04%	33.73%	37.96%	41.97%	45.44%	48.59%	51.55%	12.72
AsyFed	22.68%	27.44%	32.07%	36.19%	40.20%	43.59%	46.97%	49.64%	123.18
FedAvg	21.49%	26.13%	30.91%	35.06%	38.73%	42.14%	45.47%	48.31%	1849.80
N- τ -greedy	20.27%	24.94%	28.99%	32.73%	36.19%	38.96%	42.45%	45.07%	-

its performance is inferior to that of AsyFed. N- τ -greedy algorithm exhibits poorer performance because they are non-learning-based algorithms. Furthermore, it can be seen that the communication overhead of our scheme is much lower than that of other schemes. Compared with the traditional FedAvg and AsyFed schemes, the communication overhead is reduced by more than 98%. This is because our scheme only transmits a small amount of *HI* pairs and *KI* pairs instead of the full set of model parameters.

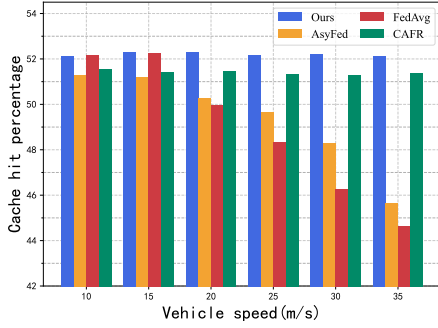


Fig. 5. Cache hit percentage versus vehicle speed.

Fig. 4 shows the changes in request content latency for various schemes under different cache capacities. It can be seen that as the cache capacity increases, the request content latency for all schemes gradually decreases. This is because a larger cache capacity makes it more likely for VUs to obtain the requested content from nearby RSU, thereby reducing the request content latency. Additionally, it can be observed that our scheme achieves the lowest request content latency, second only to Oracle. This is because our scheme has a higher cache hit percentage, making it more likely for VUs to request the content they are interested in, which reduces the request content latency.

Fig. 5 shows the maximum cache hit percentage of various schemes under different speeds. It can be seen that our scheme is hardly affected by vehicle speed. This is because our scheme trains models locally and does not require frequent interaction with RSUs; even when entering a new RSU, it can still immediately upload the content recommendation list that matches VU preferences. In addition, we also take into account the mobility characteristics of vehicles to update the cache content. CAFR is also hardly affected by changes in vehicle speed, but our scheme has better performance because we train a personalized local LDPM for each VU. As vehicle speed increases, the cache hit percentage of FedAvg and AsyFed gradually decreases. This is because vehicles leave the RSU too quickly, making it impossible to complete the training.

V. CONCLUSION

This letter addressed the challenges posed by the rapid movement of vehicles to edge caching and the issue of excessive communication overhead in model training, and proposed a federated distillation-assisted vehicle edge caching strategy based on LDPM. Finally, experiments were conducted to verify the effectiveness of the proposed algorithm.

REFERENCES

- [1] Y. Xie, Q. Wu, P. Fan, N. Cheng, W. Chen, J. Wang, and K. B. Letaief, "Resource allocation for twin maintenance and task processing in vehicular edge computing network," *IEEE Internet of Things Journal*, vol. 12, no. 15, pp. 32 008–32 021, 2025.
- [2] W. Mao, K. Xiong, Y. Lu, P. Fan, and Z. Ding, "Energy consumption minimization in secure multi-antenna uav-assisted mec networks with channel uncertainty," *IEEE Transactions on Wireless Communications*, vol. 22, no. 11, pp. 7185–7200, 2023.
- [3] Q. Wu, W. Wang, P. Fan, Q. Fan, H. Zhu, and K. B. Letaief, "Co-operative edge caching based on elastic federated and multi-agent deep reinforcement learning in next-generation networks," *IEEE Transactions on Network and Service Management*, 2024.
- [4] Y. Dong, Z. Chen, S. Liu, P. Fan, and K. B. Letaief, "Age-upon-decisions minimizing scheduling in internet of things: To be random or to be deterministic?" *IEEE Internet of Things Journal*, vol. 7, no. 2, pp. 1081–1097, 2020.
- [5] X. Di, K. Xiong, P. Fan, H.-C. Yang, and K. B. Letaief, "Optimal resource allocation in wireless powered communication networks with user cooperation," *IEEE Transactions on Wireless Communications*, vol. 16, no. 12, pp. 7936–7949, 2017.
- [6] K. Qi, Q. Wu, P. Fan, N. Cheng, W. Chen, and K. B. Letaief, "Reconfigurable-intelligent-surface-aided vehicular edge computing: Joint phase-shift optimization and multiuser power allocation," *IEEE Internet of Things Journal*, vol. 12, no. 1, pp. 764–777, 2025.
- [7] T. Li, P. Fan, Z. Chen, and K. B. Letaief, "Optimum transmission policies for energy harvesting sensor networks powered by a mobile content center," *IEEE Transactions on Wireless Communications*, vol. 15, no. 9, pp. 6132–6145, 2016.
- [8] Y. Yang, P. Fan, and Y. Huang, "Doppler frequency offsets estimation and diversity reception scheme of high speed railway with multiple antennas on separated carriages," in *2012 International Conference on Wireless Communications and Signal Processing (WCSP)*, 2012, pp. 1–6.
- [9] S. Wang, T. Tuor, T. Salonidis, K. K. Leung, C. Makaya, T. He, and K. Chan, "Adaptive federated learning in resource constrained edge computing systems," *IEEE journal on selected areas in communications*, vol. 37, no. 6, pp. 1205–1221, 2019.
- [10] H. Zhou, P. Fan, and J. Li, "Global proportional fair scheduling for networks with multiple base stations," *IEEE Transactions on Vehicular Technology*, vol. 60, no. 4, pp. 1867–1879, 2011.
- [11] Z. Yao, J. Jiang, P. Fan, Z. Cao, and V. Li, "A neighbor-table-based multipath routing in ad hoc networks," in *The 57th IEEE Semianual Vehicular Technology Conference, 2003. VTC 2003-Spring.*, vol. 3, 2003, pp. 1739–1743 vol.3.
- [12] P. Fan, C. Feng, Y. Wang, and N. Ge, "Investigation of the time-offset-based qos support with optical burst switching in wdm networks," in *2002 IEEE International Conference on Communications. Conference Proceedings. ICC 2002 (Cat. No.02CH37333)*, vol. 5, 2002, pp. 2682–2686 vol.5.
- [13] Q. Wu, Y. Zhao, Q. Fan, P. Fan, J. Wang, and C. Zhang, "Mobility-aware cooperative caching in vehicular edge computing based on asynchronous federated and deep reinforcement learning," *IEEE Journal of Selected Topics in Signal Processing*, vol. 17, no. 1, pp. 66–81, 2023.

- [14] Q. Wu and J. Zheng, "Performance modeling of ieee 802.11 dcf based fair channel access for vehicular-to-roadside communication in a non-saturated state," in *2014 IEEE International Conference on Communications (ICC)*. IEEE, 2014, pp. 2575–2580.
- [15] Z. Yu, J. Hu, G. Min, Z. Zhao, W. Miao, and M. S. Hossain, "Mobility-aware proactive edge caching for connected vehicles using federated learning," *IEEE Transactions on Intelligent Transportation Systems*, vol. 22, no. 8, pp. 5341–5351, 2020.
- [16] O. Ronneberger, P. Fischer, and T. Brox, "U-net: Convolutional networks for biomedical image segmentation," in *Medical image computing and computer-assisted intervention–MICCAI 2015: 18th international conference, Munich, Germany, October 5–9, 2015, proceedings, part III 18*. Springer, 2015, pp. 234–241.
- [17] Z. Kong, W. Ping, J. Huang, K. Zhao, and B. Catanzaro, "Diffwave: A versatile diffusion model for audio synthesis," *arXiv preprint arXiv:2009.09761*, 2020.
- [18] V. Popov, I. Vovk, V. Gogoryan, T. Sadekova, and M. Kudinov, "GradTts: A diffusion probabilistic model for text-to-speech," in *International conference on machine learning*. PMLR, 2021, pp. 8599–8608.
- [19] J. Ho, A. Jain, and P. Abbeel, "Denoising diffusion probabilistic models," *Advances in neural information processing systems*, vol. 33, 2020.
- [20] R. Rombach, A. Blattmann, D. Lorenz, P. Esser, and B. Ommer, "High-resolution image synthesis with latent diffusion models," in *Proceedings of the IEEE/CVF conference on computer vision and pattern recognition*, 2022, pp. 10 684–10 695.
- [21] Z. Wu, S. Sun, Y. Wang, M. Liu, K. Xu, W. Wang, X. Jiang, B. Gao, and J. Lu, "Fedcache: A knowledge cache-driven federated learning architecture for personalized edge intelligence," *IEEE Transactions on Mobile Computing*, vol. 23, no. 10, pp. 9368–9382, 2024.
- [22] Y. A. Malkov and D. A. Yashunin, "Efficient and robust approximate nearest neighbor search using hierarchical navigable small world graphs," *IEEE transactions on pattern analysis and machine intelligence*, vol. 42, no. 4, pp. 824–836, 2018.
- [23] Z. Shao, Q. Wu, P. Fan, N. Cheng, Q. Fan, and J. Wang, "Semantic-aware resource allocation based on deep reinforcement learning for 5g-v2x hetnets," *IEEE Communications Letters*, vol. 28, no. 10, pp. 2452–2456, 2024.
- [24] S. Müller, O. Atan, M. Van Der Schaar, and A. Klein, "Context-aware proactive content caching with service differentiation in wireless networks," *IEEE Transactions on Wireless Communications*, vol. 16, no. 2, pp. 1024–1036, 2016.